

INFLUENCE OF NOTCH (TIP) RADIUS ON FATIGUE CRACK GROWTH RATE

DARIUSZ ROZUMEK
EWALD MACHA

Faculty of Mechanical Engineering, Technical University of Opole, Poland
e-mail: drozumek@po.opole.pl; emac@po.opole.pl

PAOLO LAZZARIN

Department of Management and Engineering, University of Padova, Vicenza, Italy
e-mail: plazzarin@gest.unipd.it

GIOVANNI MENEGHETTI

Department of Mechanical Engineering, University of Padova, Padova, Italy
e-mail: meneghetti@unipd.it

The paper deals with the problem of fatigue crack propagation from notches in plates made of FeP04 steel and AA356-T6 aluminium alloy. The tests were performed under different stress ranges by keeping the nominal load ratio ($R = 0.1$) constant. The specimens were weakened by nearly-sharp and blunt two-sided notches. The results of the fatigue tests were then reanalysed in terms of the J-integral range including influence of the notch. It was observed that the blunter notches are, the higher fatigue crack growth rate is.

Key words: fatigue crack growth, J-integral range, load ratio, notch

Notations

E	–	Young's modulus
K_t	–	stress concentration factor
K'	–	cyclic strength coefficient
P_a	–	amplitude of load
R	–	load ratio

a	–	crack length
b	–	fatigue strength exponent
c	–	fatigue ductility exponent
d	–	notch depth
da/dN	–	fatigue crack growth rate
n'	–	cyclic strain hardening exponent
t	–	specimen thickness
w	–	specimen width
ΔJ_I	–	integral range
ΔK_I	–	stress intensity factor range
ε'_f	–	fatigue ductility coefficient
ν	–	Poisson's ratio
ρ	–	notch tip radius
σ_{nom}	–	nominal stress
σ_{TS}	–	ultimate tensile strength
σ_Y	–	yield stress
σ'_f	–	fatigue strength coefficient

1. Introduction

Whenever fatigue loading occurs, stress concentrations or notches, no matter macroscopic or microscopic, are preferred sites for crack initiation. Thus, the notch shape determines, as well known, the fatigue limit of the component (Macha and Rozumek, 2003). Recently, a diagram has been proposed in which the fatigue limit of the notched component was predicted on the basis of either the theoretical stress concentration factor K_t or the stress intensity factor range ΔK_{th} , with the notch modelled as a crack of the equivalent depth (Atzori *et al.*, 2003).

In the low-medium fatigue range, the fatigue life is usually thought of as a sum of fatigue crack initiation and fatigue crack propagation, although the differentiation of the two stages is qualitatively distinguishable but quantitatively ambiguous (Jiang and Feng, 2004). Residual fatigue life calculations are carried out by means of $da/dN - \Delta K$ curves obtained from conventional, pre-cracked specimens, often considering the fatigue growth rate as independent of the notch shape. However, when a fatigue crack is initiated from a notch, the crack propagation rate is generally higher than that expected by using the stress intensity factor, mainly because tip there exists a prior accumulation of fatigue damage in initiating the fatigue crack ahead of the notch (Jiang and Feng, 2004).

In the presence of non-localised yielding, the parameter ΔK is no longer applicable and an energetic approach based on the J-integral (Rice, 1968) might be a more appropriate choice, mainly because local and global changes of the energy occur during fatigue loading. In paper by El Haddad *et al.* (1980), behaviour of small fatigue cracks was analysed and described with use of the stress intensity factor range and J-integral. The tests were done in elastic and plastic ranges on smooth specimens with blunt notches. The J-integral was applied for the description of plastic changes appearing near the notch. It was found that the J-integral is a good parameter for describing changes occurring in various notches. In the paper by Ogura *et al.* (1987), behaviour of the effective fatigue crack growth in notched elements was investigated. For the description of test results, ΔK_{eff} and ΔJ_{eff} parameters were used. It was concluded that ΔK_{eff} is the most important parameter for the description of the fatigue crack growth for small cracks at the notch root. It was also found that ΔJ_{eff} is a suitable parameter to be applied in the case of appearance of a plastic zone at the notch root and for small cracks.

The main aim of this paper is characterisation of fatigue crack growth rates in terms of the ΔJ -integral, by using experimental data from plates of two different materials, weakened by rounded and nearly-sharp notches.

2. Materials and test procedure

2.1. Static properties and strain-based cyclic tests

Present re-analyses are based on sets of experimental data already reported in the literature (Lazzarin *et al.*, 1997). Tests were carried out on plates made of FeP04-UNI 8092 deep-drawing steel and AA356-T6 cast aluminium alloy, weakened by symmetric lateral notches of varying acuity. For static and fatigue tests, a Schenck PSA100 servo-hydraulic device was used at the Department of Mechanical Engineering of the Padova University. Elastic and static properties of the two materials are summarised in Table 1.

Table 1. Elastic and static strength properties

Materials	σ_Y [MPa]	σ_{TS} [MPa]	E [GPa]	ν
FeP04 steel	185	310	191	0.30
AA356-T6 aluminium alloy	182	250	71	0.32

Strain-based fatigue curves are shown in Fig. 1, where elastic and plastic components are given too, together with the best fitting values of the material properties. As usual, such curves are described by a linear law in a log-log diagram as suggested by the Manson - Coffin model. In the same figures, some stabilised hysteresis loops are displayed too. Coefficients of the Ramberg-Osgood equation describing the cyclic strain curve under tension-compression conditions with $R_\epsilon = -1$ (a Schenck extensometer was used with a gauge length equal to 25 mm) for FeP04 steel and AA356-T6 aluminium alloy were presented in Fig. 1 (Lazzarin *et al.*, 1997).

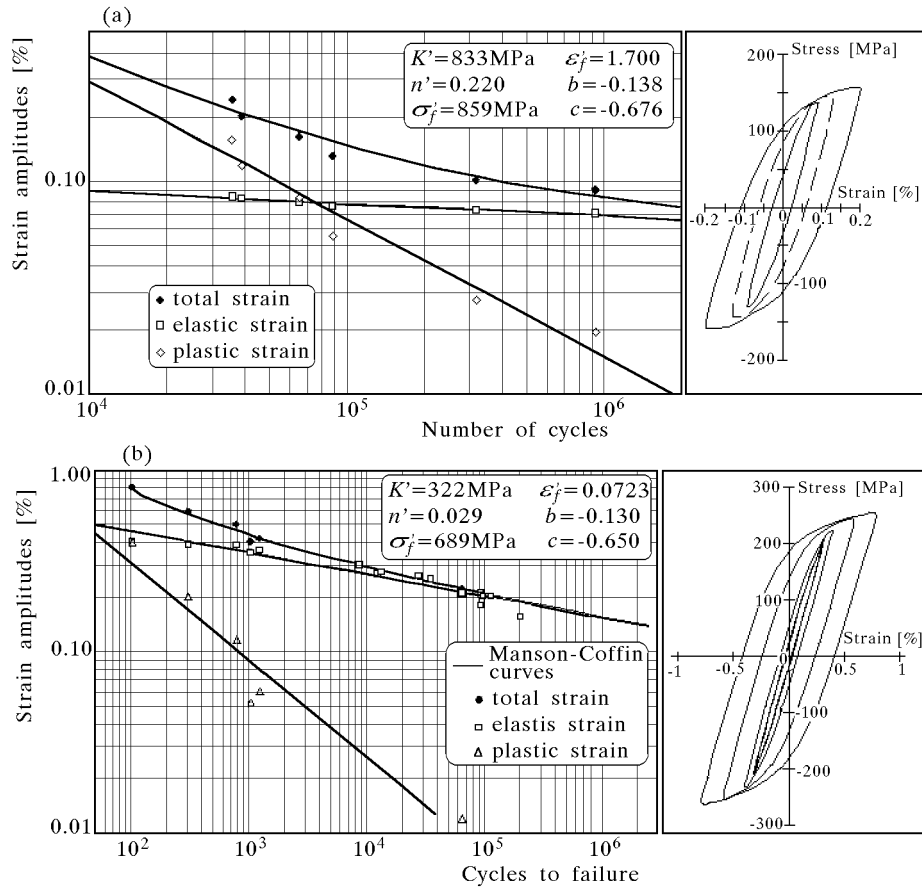


Fig. 1. Fatigue curves under strain control and some stabilised hysteresis loops;
 (a) FeP04, (b) AA356-T6

2.2. Fatigue tests of notched specimens

All fatigue tests were carried out under load control by imposing a constant value of the nominal load ratio, $R = 0.1$, and a frequency ranging from 20 to 25 Hz. The specimens were characterised by double symmetric lateral notches with a notch root radius ranging from 0.1–0.2 mm to 10 mm (Fig. 2 and Table 2).

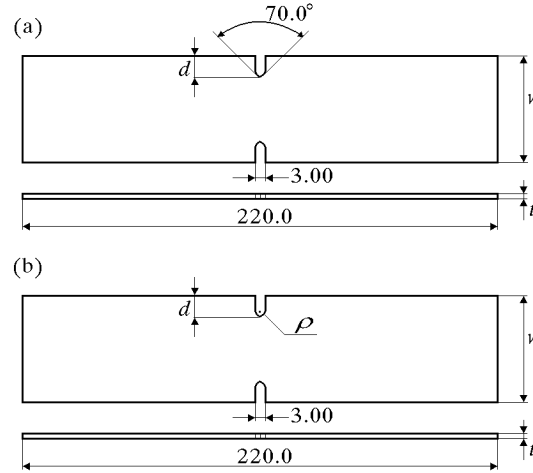


Fig. 2. Geometry of specimens characterised by: (a) sharp and (b) blunt notches. All dimensions in mm

The endurance limit for plain specimens was $\Delta\sigma_0 = 247$ MPa at 2 million cycles for FeP04 and 140 MPa for AA356-T6. For the notched specimens the endurance limits $\Delta\sigma_{A,g}$ at $N_A = 2 \cdot 10^6$ cycles are summarized in Table 2, together with theoretical stress concentration factors evaluated by FE analyses. $K_{t,g}$ and $\Delta\sigma_{A,g}$ in Table 2 is referred to the gross area of the specimens.

Table 2. Geometrical parameters, stress concentration factors and fatigue strength range of notch specimens ($K_{t,g}$ and $\Delta\sigma_{A,g}$ referred to the gross area, subscript g)

Materials	d [mm]	w [mm]	t [mm]	ρ [mm]	$K_{t,g}$	$\Delta\sigma_{A,g}$ [MPa] at $2 \cdot 10^6$ cycles
FeP04 steel	10	50	2	0.2	16.3	51.7
				2.5	5.38	63.0
				10	3.07	90.0
AA356-T6 aluminium alloy	8	40	4	0.1	20.2	29.2
				2.5	4.92	39.9

In a number of fatigue tests, fatigue crack initiation and propagation phases are controlled by means of a stereoscope ($64\times$). The surfaces of the specimens, 40-50 mm wide, were accurately polished in order to make cracks originated from the notch tip easily distinguishable. In Lazzarin *et al.* (1997), a crack was considered "significant" when its length was equal to a_0 , by using for a_0 the definition given in (El Haddad *et al.*, 1979). For a low-carbon steel, with $\Delta\sigma_A = 247$ MPa and $\Delta K_{th,0} \cong 10$ MPa \cdot m $^{1/2}$ (both values referring to a nominal ratio R close to zero), the material length parameter a_0 resulted to be 0.5 mm. On the other hand, considering average values of thresholds among those reported in the literature concerning cast light alloys ($\Delta K_{th,0} \cong 5$ MPa \cdot m $^{1/2}$) in combination with $\Delta\sigma_A = 140$ MPa, a_0 was 0.41 mm. In Lazzarin *et al.* (1997), the demarcation line between fatigue crack initiation and propagation phases was conventionally drawn just in correspondence of a_0 . Such a threshold length was found to be the limit value beyond which cracks became through-thickness and their propagation began to be sufficiently stable. This was not true in some light alloy specimens where, due to greater thickness and material porosity, a number of different corner and surface microcrack initiation sites were detected, thus resulting in higher scatter of fatigue strength properties.

3. Experimental results

Some plots of the crack length a versus the number of cycles N for FeP04 and AA356-T6 are shown in Fig. 3. Different symbols are used depending on the notch root ρ . The specimens were subjected to cyclic tension at constant amplitudes of load:

- FeP04 – $P_a = 3.9$ kN for $\rho = 0.2$ mm, $P_a = 4.2$ kN for $\rho = 2.5$ mm and $P_a = 5.4$ kN for $\rho = 10$ mm, corresponding to the nominal stress range amplitude to crack initiation $\Delta\sigma_{nom} = 145$ MPa for $\rho = 0.2$ mm, $\Delta\sigma_{nom} = 156$ MPa for $\rho = 2.5$ mm and $\Delta\sigma_{nom} = 200$ MPa for $\rho = 10$ mm
- AA356-T6 – $P_a = 4.8$ kN for $\rho = 0.2$ mm and $P_a = 6.72$ kN for $\rho = 2.5$ mm, corresponding to the nominal stress range amplitude to crack initiation $\Delta\sigma_{nom} = 50$ MPa for $\rho = 0.2$ mm and $\Delta\sigma_{nom} = 70$ MPa for $\rho = 2.5$ mm.

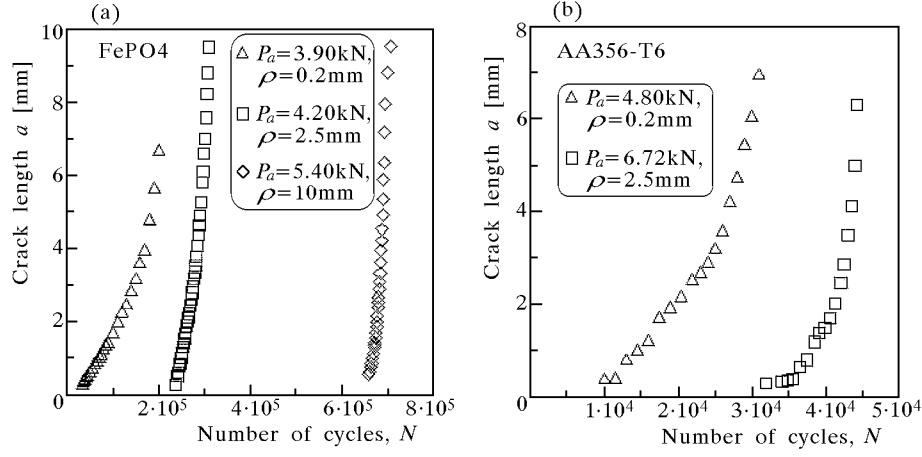


Fig. 3. Crack length as a function of the number of cycles; (a) FePO4, (b) AA356-T6

Afterwards, the fatigue crack growth rate was evaluated according with the following equation (Dowling and Begley, 1976)

$$\frac{da}{dN} = B(\Delta J_I)^n \quad (3.1)$$

where $\Delta J_I = J_{max} - J_{min}$, and the parameters B and n need a best-fit analysis. ΔJ_I in Eq. (3.1) was calculated by using the following relationship (Rozumek, 2004)

$$\Delta J_I = \frac{\Delta K_I^2}{E} + \pi Y^2 \frac{\Delta \sigma \Delta \varepsilon_p a}{\sqrt{n'}} \quad (3.2)$$

where a is the crack length, $Y = Y_1 Y_2$ a correction factor and $\Delta \sigma$ is the stress range corresponding to the plastic strain range $\Delta \varepsilon_p$, both ranges evaluated ahead of the notch.

In order to include the influence of crack length to gross area ratio as well as the non-uniform stress distribution due to notches, the stress intensity factor range was evaluated from the following expression

$$\Delta K_I = Y_1 Y_2 \Delta \sigma_{nom} \sqrt{\pi(a+d)} \quad (3.3)$$

where $\Delta \sigma_{nom}$ is evaluated on the gross area, and coefficients Y_1 and Y_2 are (other symbols in Fig. 4)

$$Y_1 = 1.12 + 0.203 \frac{2(a+d)}{w} - 1.197 \left(\frac{2(a+d)}{w} \right)^2 + 1.930 \left(\frac{2(a+d)}{w} \right)^3$$

$$Y_2 = \sqrt{1 - e^{-\beta}} \quad \text{with} \quad \beta = \frac{6a(\rho + w - 2d)}{\rho(w - 2d)}$$

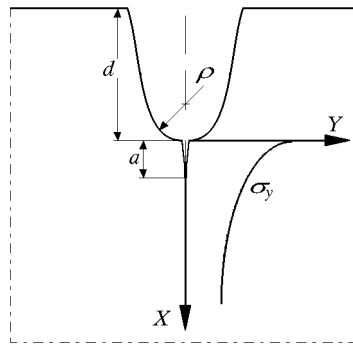


Fig. 4. Description of symbols used for estimation of the range of stress intensity factors

The coefficient Y_2 was determined in Lazzarin *et al.* (1997) by means of a number of ad hoc FE analyses. Results from Eq. (3.3) are plotted in Fig. 5. The effect of the non-uniform stress distribution due to different notch root radii on ΔK_I is evident there.

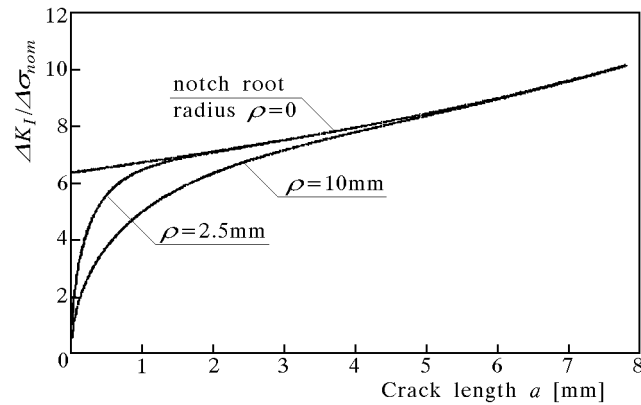


Fig. 5. Stress intensity factor range for different values of the notch root radius, see Eq. (3.3)

Curves of the fatigue crack growth rate versus the J-integral range for steel and aluminium alloys are plotted in Fig. 6. Plots 1a, 1b and 1c in Fig. 6a make it clearly seen that the fatigue crack growth rate increases as the root radius ρ increases. It is especially visible at the final stage of cracking, for example for $\Delta J = 5 \cdot 10^{-2}$ MPa·m under a change of the notch root radius from 0.2 mm to 10 mm, the crack growth rate increases three times. This fact may be caused by a longer initiation period characterising specimens with blunt notches, accomplished by major local damage ahead of notches before of the appearance of a fatigue crack.

Moreover, comparing the two tested materials, a higher fatigue crack growth rate was noticed in the AA356-T6 aluminium alloy. In Fig. 6, graph 1 is related to averaged values of the coefficients B and n found from Eq. (3.1).

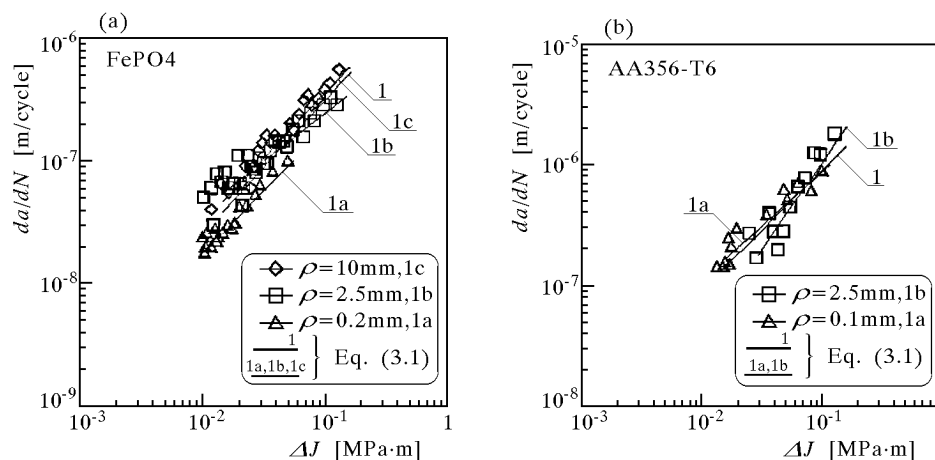


Fig. 6. A comparison between experimental results and values calculated according to Eq.(3.1); (a) FeP04, (b) AA356-T6

Table 3. Coefficients B and n , Eq. (3.1), and correlation index r for curves in Fig. 6

Materials	Figures Graphs	B [m/(MPa·m) ^{n} cycle]	n	r
FeP04	Fig. 6a - 1	$4.344 \cdot 10^{-6}$	1.099	0.921
	Fig. 6a - 1a	$2.274 \cdot 10^{-6}$	1.041	0.969
	Fig. 6a - 1b	$1.583 \cdot 10^{-6}$	0.782	0.926
	Fig. 6a - 1c	$4.541 \cdot 10^{-6}$	1.062	0.975
AA356-T6	Fig. 6b - 1	$9.683 \cdot 10^{-6}$	0.995	0.912
	Fig. 6b - 1a	$7.523 \cdot 10^{-6}$	0.899	0.959
	Fig. 6b - 1b	$3.261 \cdot 10^{-5}$	1.441	0.923

In the elastic-plastic range, stresses and strains were calculated by means of the finite element program FRANC2D. In the models, six-node triangular elements were used. In Fig. 6, plots 1a, 1b for the AA356-T6 aluminium alloy show a trend similar to that of the FeP04 steel. The coefficients B and n , as well as the correlation index r , were determined with the least square method for a confidence level $\alpha = 0.05$. All coefficients are listed in Table 3, where

some variations of the coefficients B and n depending on the notch type are evident. High values of the correlation coefficient r clearly demonstrate that the correlation between test results and the assumed model is significant.

4. Conclusion

The results of fatigue crack growth tests on notched specimens made of FeP04 steel and AA356-T6 aluminium alloy tested under tension loading, allow the following conclusions to be drawn:

- In elastic-plastic materials, the notch type strongly influences both the initial value of J-integral range and the shape of crack growth rate curves.
- In notched specimens made of the FeP04 steel and in the presence of a nominal load ratio $R = 0.1$, the greater was the radius of a notch root, the greater the was fatigue crack growth rate.
- Comparing the two materials, a higher crack growth rate was found in the AA356-T6 aluminium alloy with respect to the FeP04 steel.

Acknowledgements

This work was supported by the Commission of the European Communities under the FP5, GROWTH Programme, contract No. G1MA-CT-2002-04058 (CESTI).

References

1. ATZORI B., LAZZARIN P., MENEGHETTI G., 2003, Fracture mechanics and notch sensitivity, *Fatigue and Fracture of Engineering Materials and Structures*, **26**, 257-267
2. DOWLING N.E., BEGLEY J.A., 1976, Fatigue crack growth during gross plasticity and the J-integral, In: *Mechanics of Crack Growth*, ASTM STP 590, American Society for Testing and Materials, 82-103
3. EL HADDAD M.H., DOWLING N.E., TOPPER T.H., SMITH K.N., 1980, J-integral applications for short fatigue cracks at notches, *International Journal of Fracture*, **16**, 15-30
4. EL HADDAD M.H., TOPPER T.H., SMITH K.N., 1979, Prediction of non-propagating cracks, *Engineering Fracture Mechanics*, **11**, 573-584

5. JIANG Y., FENG M., 2004, Modelling of fatigue crack propagation, *Journal of Engineering Materials and Technology*, **126**, 77-86
6. LAZZARIN P., TOVO R., MENEGHETTI G., 1997, Fatigue crack initiation and propagation phases near notches in metals with low notch sensitivity, *International Journal of Fatigue*, **19**, 647-657
7. MACHA E., ROZUMEK D., 2003, Fatigue crack path development in a one-sided restrained bar with a rectangular section and stress concentrator under bending, *Proc. Int. Conference on Fatigue Crack Paths (FCP 2003)*, Parma, CD-ROM, 8 ps
8. OGURA K., MIYOSHI Y., NISHIKAWA I., 1987, Fatigue crack growth and closure of small cracks at the notch root, *Current Research on Fatigue Cracks*, Ed. Tanaka T. *et al.*, Elsevier Applied Science, London and New York, **1**, 67-91
9. RICE J.R., 1968, A path independent integral and the approximate analysis of strain concentration by notches and cracks, *Journal of Applied Mechanics*, **35**, 379-386
10. ROZUMEK D., 2004, The ΔJ -integral range applied for the description of fatigue crack growth rate, *Proc. 12th Int. Conference on Experimental Mechanics (ICEM12)*, Bari, 275-276 and CD-ROM, 8 ps

Wpływ promienia (wierzchołka) karbu na prędkość wzrostu pęknięć zmęczeniowych

Streszczenie

W pracy przedstawiono propagację pęknięć zmęczeniowych, w próbkach płaskich z korbami, wykonanych ze stali FeP04 i stopu aluminium AA356-T6. Badania wykonywano przy różnych zakresach naprężeń i stałym współczynniku asymetrii cyklu ($R = 0.1$). Próbki były osłabione przez dwustronne ostre i łagodne karby. Wyniki badań zmęczeniowych opisano za pomocą zakresu całki J z uwzględnieniem wpływu karbu. Stwierdzono, że im łagodniejszy karb, tym większa prędkość wzrostu pęknięć zmęczeniowych.

Manuscript received July 13, 2005; accepted for print September 5, 2005